# GC-MSC-derived circ_0024107 promotes gastric cancer cell lymphatic metastasis via fatty acid oxidation metabolic reprogramming mediated by the miR-5572/6855-5p/CPT1A axis

LIN WANG[1*], CHEN WU[1*], JUAN XU[2*], ZHEN GONG[1], XIAOLI CAO[3], JIAYING HUANG[1], HAIBO DONG[4], WEI ZHU[1], FENG HUANG[1,5,6], CHENGLIN ZHOU[2] and MEI WANG[1]

[1]Department of Laboratory Medicine, School of Medicine, Jiangsu University, Zhenjiang, Jiangsu 212013; [2]Department of Laboratory Medicine, The Affiliated Taizhou People's Hospital of Nanjing Medical University, Taizhou, Jiangsu 225300; [3]Department of Laboratory Medicine, Affiliated Tumor Hospital of Nantong University, Nantong, Jiangsu 226001; [4]Department of Hematology, Nanjing Drum Tower Hospital, Affiliated Hospital of Jiangsu University, Nanjing, Jiangsu 210008; [5]Department of Clinical Laboratory, Affiliated Kunshan Hospital of Jiangsu University, Suzhou, Jiangsu 215300; [6]Department of Clinical Laboratory, Maternal and Child Health Care Hospital of Kunshan, Suzhou, Jiangsu 215300, P.R. China

Received January 11, 2023; Accepted May 4, 2023

DOI: 10.3892/or.2023.8575

**Abstract.** Gastric cancer tissue-derived mesenchymal stem cells (GC-MSCs) play a critical role in facilitating gastric cancer metastasis. Recently, circular RNAs (circRNAs) and metabolic reprogramming have been found to be extensively involved in the malignant progression of tumors, including gastric cancer. However, the biological role and potential mechanisms of GC-MSC-derived circRNAs in metabolic reprogramming remain elusive. Herein, the expression profiles of circRNAs and mRNAs were compared between GC-MSCs and bone marrow-derived MSCs (BM-MSCs) using microarray analysis. circ_0024107 was identified to mediate GC-MSCs to promote gastric cancer lymphatic metastasis by inducing fatty acid oxidation (FAO) metabolic reprogramming. Mechanistically, circ_0024107 served as a sponge of miR-5572 and miR-6855-5p to elicit the FAO metabolic reprograming of GC-MSCs by upregulating carnitine palmitoyltransferase 1A (CPT1A). In addition, GC-MSCs promoted metastasis which was dependent on the induction of FAO in gastric cancer cells mediated by circ_0024107. The circ_0024107/miR-5572/6855-5p/CPT1A axis was deregulated in gastric cancer tissues and GC-MSCs, and was associated with lymph node metastasis and the prognosis of patients with gastric cancer. Taken together, the findings of the present study suggest the crucial role of FAO metabolic reprogramming mediated by GC-MSC-derived circ_0024107 in synergistically promoting gastric cancer lymphatic metastasis via miR-5572/6855-5p-CPT1A signaling; this suggests that circ_0024107 may be an attractive target for gastric cancer intervention.

*Correspondence to:* Professor Mei Wang, Department of Laboratory Medicine, School of Medicine, Jiangsu University, 301 Xuefu Road, Zhenjiang, Jiangsu 212013, P.R. China
E-mail: wangmei8417@163.com

Professor Chenglin Zhou, Department of Laboratory Medicine, The Affiliated Taizhou People's Hospital of Nanjing Medical University, 210 Yingchun Road, Taizhou, Jiangsu 225300, P.R. China
E-mail: 18762340015@njmu.edc.cn

*Contributed equally

*Key words:* tumor microenvironment, mesenchymal stem cells, circular RNA, lymph node metastasis, gastric cancer

## Introduction

Gastric cancer remains a serious threat to human health, with its incidence and mortality ranking fifth and fourth globally, respectively (1). Cancer sustains its proliferative and metastatic capacities depending on its surrounding microenvironment, which renders tumor stromal cells attractive therapeutic targets for cancer (2). Previously, our research group successfully obtained and identified mesenchymal stem cell-like cells (MSCs) from primary gastric cancer tissues (GC-MSCs) (3), and demonstrated that these stromal cells directly promote gastric cancer cell proliferation, migration, invasion and cancer stem cell properties (4-7). These cells also create an immunosuppressive microenvironment for immune escape by disrupting the Treg/Th17 balance, inducing M2-like macrophage polarization, and impairing $CD8^+$ T-cell antitumor activity (8-10). GC-MSCs represent a promising intervention target for the treatment of gastric cancer. The exploration of GC-MSC-derived abnormal molecules may be crucial for uncovering the underlying mechanisms of gastric cancer progression.

Emerging evidence indicates that circular RNAs (circRNAs) and metabolic reprogramming are two critical

research hotspots in the field of cancer. CircRNAs are non-coding RNAs that are characterized by their covalently closed circular structure. To date, a large number of circRNAs have been screened and identified in gastric cancer cells, tissues and plasma through high-throughput sequencing technologies and bioinformatics analyses. It is clear that circRNAs play either oncogenic or tumor-suppressive roles, and hold promise as diagnostic, prognostic biomarkers and therapeutic targets for gastric cancer (11,12). However, circRNA expression profiles, function and regulatory mechanisms in gastric cancer-associated stromal cells remain elusive. Metabolic reprogramming is one of the hallmarks of cancer. Previous studies have suggested that metabolic alteration is not unique to cancer cells, and immune cells undergo metabolic changes to impair their antitumor immunity, thus forming an immunosuppressive microenvironment to support gastric cancer progression (13,14). Notably, a recent bioinformatics analysis demonstrated that the metabolic reprogramming signature of stromal cells could be explored to calculate prognosis risk scores, which had good a performance in predicting the overall survival (OS) of patients with gastric cancer (15). This finding highlights the critical role of the metabolic reprogramming of stromal cells in gastric cancer. However, the metabolic reprogramming of stromal cells and the mechanisms responsible for the promotion of gastric cancer metastasis remain unclear.

The present study investigated aberrant circRNAs and metabolic disorders in GC-MSCs, explored the role and mechanisms of circRNAs in modulating the metabolic reprogramming of GC-MSCs and determined the clinical significance of the circRNA-regulatory axis in gastric cancer. It is hoped that the findings presented herein may help to uncover a novel mechanism and provide a potential therapeutic strategy for gastric cancer from the perspective of the circRNA mediated-metabolic reprogramming of GC-MSCs.

## Materials and methods

*Cell culture, conditioned medium (CM) preparation and etomoxir treatment.* Bone marrow-derived MSCs (BM-MSCs), GC-MSCs, and gastric cancer cell lines AGS (cat. no. TCHu232, The Cell Bank of Type Culture Collection of the Chinese Academy of Sciences) and HGC-27 (cat. no. TCHu22, The Cell Bank of Type Culture Collection of the Chinese Academy of Sciences) were obtained and cultured as previously described (3,16). Briefly, fresh gastric cancer tissues were washed with phosphate-buffered saline (PBS), cut into 1-$mm^3$-sized pieces and floated in DMEM with low glucose (LG-DMEM) (Invitrogen; Thermo Fisher Scientific, Inc.) containing 10% FBS, penicillin and streptomycin. The tissue pieces were subsequently incubated at 37˚C in humid air with 5% $CO_2$, and the medium was replaced every 3 days after the initial plating. When adherent fibroblast-like cells appeared after 10 days of culture, the cells were trypsinized and passaged into a new flask for further expansion. When these cells reached confluence at the third passage, a homogeneous cell population was obtained and used for the subsequent experiments. The collection of tissues from gastric cancer patients was approved by the Affiliated Tumor Hospital of Nantong University (approval no. 2021-017). Informed consent was obtained from all patients prior to surgery. MSC-CM was prepared as previously specified (8). When the MSC confluency reached ~60%, the cells were washed with PBS (Gibco; Thermo Fisher Scientific, Inc.) and incubated with DMEM (Gibco; Thermo Fisher Scientific, Inc.) containing 10% FBS (Biological Industries Israel Beit Haemek Ltd.). After 48 h, the MSC-CM was harvested separately, centrifuged at 300 x g for 5 min, at 4˚C, and filtered through a 0.45-$\mu$m membrane (cat. no. SLFH050, Merck KGaA). The final CM was stored at -20˚C. The MSCs and gastric cancer cells were attached overnight and treated with etomoxir (cat. no. HY-50202, MedChemExpress) at final concentrations of 100 and 40 $\mu$M for 24 h, respectively. The MSCs were then subjected to transfection (as described below), while the gastric cancer cells were further treated with MSC-CM for subsequent analyses.

*Clinical tissues.* A total of 40 gastric cancer tissues and paired adjacent non-cancerous tissues were provided by the Affiliated Tumor Hospital of Nantong University from March, 2021 to October, 2022 (Nantong, China). All the obtained tissues were independently diagnosed by two pathologists and stored at -80˚C. None of the patients had received any therapy prior to surgery. The collection of tissues from gastric cancer patients was approved by the Affiliated Tumor Hospital of Nantong University (approval no. 2021-017). Informed consent was obtained from all patients prior to surgery.

*RNA extraction and reverse transcription-quantitative PCR (RT-qPCR).* Total RNA was extracted from clinical tissues and cell lines using TRIzol® reagent (Invitrogen; Thermo Fisher Scientific, Inc.). Reverse transcription reactions were performed using the PrimeScript™ RT reagent kit (Takara Bio, Inc.) using random primers and oligo dT primers for circRNA and mRNA detection, respectively, as well as specific stem-loop primers (GenePharma Co., Ltd.) for miRNA detection. qPCR was carried out using TB Green® Premix Ex Taq™ II (Takara Bio, Inc.) on the Bio-Rad fluorescence thermal cycler CFX-96 (Bio-Rad Laboratories, lnc.) with β-actin or U6 as internal controls. The PCR cycle conditions were an initial denaturation at 95˚C for 10 min; 40 cycles of 94˚C 30 sec, 60˚C 30 sec and 72˚C 30 sec; and a final extension at 72˚C for 1 min. The relative RNA expression levels were determined using the $2^{-\Delta\Delta Cq}$ method (17). The primers for circRNA and mRNA detection are presented in Table SI. miRNA primers were purchased from GenePharma Co., Ltd.

*RNase R treatment and subcellular fractionation assay.* For RNA digestion assay, 2 $\mu$g RNA isolated from GC-MSCs were mixed with RNase R (Epicentre; Illumina, Inc.) and incubated at 37˚C for 20 min. Cytoplasmic and nuclear RNA were separately obtained from the GC-MSCs using the PARIS™ kit (Invitrogen; Thermo Fisher Scientific, Inc.) following the manufacturer's protocol. The relative expression of RNA in the two fractions was detected using RT-qPCR. U6 and β-actin were used as controls to evaluate the efficiency of subcellular fractionation isolation.

*Microarray analysis*. Microarray analysis was conducted by Shanghai Biotechnology Corporation using SBC Human (4x180K) ceRNA array (Agilent Technologies, Inc.). In brief, total RNA was extracted, purified and examined for a RIN number. The RNA was then amplified and labeled. Each slide was hybridized with Cy3-labeled cRNA, washed in staining dishes and then scanned. Raw data were normalized using the Quantile algorithm, limma packages in R. The threshold value for significance that was used to define upregulation or downregulation was a fold change >2 and P<0.05.

*circRNA overexpression plasmid construction, oligonucleotides and cell transfection*. Human circ_0024107 cDNA was amplified and cloned into the GV486 vector by Genechem (Shanghai Genechem Co., Ltd.). The corresponding empty vector was used as the control. Two small interfering RNA (siRNA) duplexes targeting the back-splice junction of circ_0024107, miRNA mimics, miRNA inhibitor and corresponding negative controls were designed and purchased from GenePharma Co., Ltd. and were transiently transfected into the MSCs using Lipofectamine 2000® (Invitrogen, Thermo Fisher Scientific, Inc.). siRNAs and inhibitor were transfected at a final concentration of 100 nM, while mimics were transfected at a final concentration of 5 nM. A total of 1 $\mu$g of the plasmid was transfected into MSCs per well in a six-well plate. After 4 to 6 h, the cells were washed with PBS and refreshed with DMEM containing 10% FBS. After 48 h, the cell supernatant was collected, centrifuged at 1,000 x g at 4˚C for 20 min, filtered and finally stored at -20˚C until use. The transfection efficiency was determined using RT-qPCR and western blot analysis. The sequences of these oligonucleotides are presented in Table SII.

*Transwell assay, carnitine palmitoyltransferase 1 (CPT1) activity and β-oxidation rate detection*. Migration and invasion were examined using Transwell assays, and CPT1 activity and β-oxidation rate detection were conducted as previously described (16,18). Briefly, $8x10^4$ gastric cancer cells suspended in serum-free culture media (Gibco; Thermo Fisher Scientific, Inc.) were plated into the upper chambers of Transwell inserts (Corning, USA) with or without pre-coating with Matrigel (BD Biosciences), and separately incubated with the bottom chambers containing fresh cell culture media (Gibco; Thermo Fisher Scientific, Inc.) for 10 and 24 h at 37˚C for migration and invasion assays. The cells were fixed with 4% paraformaldehyde at room temperature for 30 min, and stained with 4% crystal violet (Beyotime Institute of Biotechnology) for 15 min. A light microscope (Nikon Corporation) was used to observe the cells. For CPT1 activity and β-oxidation rate assays, cell mitochondria were isolated and separately subjected to detection using a CPT1 Spectrophotometric Detection kit (Zikerbio) and the Fatty Acid β-oxidation Rate Colorimetric Assay kit (Genmed Scientifics, Inc.) as per the manufacturers' instructions.

*Animal tumor model*. Male BALB/c nude mice (4 weeks old; 5 mice per group) were housed in a pathogen-free facility (26˚C; 50% humidity; with food and water provided *ad libitum*) at the Animal Center of Jiangsu University and randomly divided into two groups, including the si-circ_0024107 group injected with HGC-27 cells subjected to circ_0024107 silencing-GC-MSC-CM and the NC group inoculated with HGC-27 cells pre-treated with negative control oligonucleotide-infected GC-MSC-CM. A total of $2x10^6$ HGC-27 cells were suspended in 200 $\mu$l PBS and injected into the left footpads of the nude mice to establish animal models of lymph node metastasis. After 3 to 4 weeks, the draining popliteal lymph nodes became swollen and there were palpable lumps, and the mice were then sacrificed by cervical dislocation, and the draining popliteal and inguinal lymph nodes were harvested for imaging, weighing and immunohistochemical staining. The animal experiment was approved by the Committee on Use and Care of Animals of Jiangsu University [approval no. SYXK(Su) 2018-0053].

*Western blot analysis*. Cellular proteins were extracted from the cells using RIPA lysis buffer pre-mixed with protease and phosphatase inhibitors (Beyotime Institute of Biotechnology). The concentration of proteins were determined using a BCA Protein Assay kit (cat. no. CW0014S, Beijing Kangwei Century Biotechnology Co., Ltd.) and the mass of protein loaded per lane was 8 $\mu$g. The PVDF membranes bearing proteins were blocked using 5% BSA at room temperature for 1 h and then immersed in 5% BSA containing primary antibody against CPT1A (cat. no. ab128568, dilution: 1:1,000, Abcam) and β-actin (cat. no. AC038, dilution: 1:50,000, ABclonal Biotech Co., Ltd.) overnight at 4˚C followed by incubation with the corresponding secondary antibody at 37˚C. The secondary antibodies HRP-conjugated-goat anti-mouse IgG (H+L) (cat. no. AS003, ABclonal Biotech Co., Ltd.) and HRP-conjugated-goat anti-rabbit IgG (H+L) (cat. no. AS014, ABclonal Biotech Co., Ltd.) were used at a dilution of 1:5,000. β-actin was used as the loading control. Signaling was detected using ECL Substrate (Bio-Rad Laboratories, Inc.).

*Immunohistochemical staining*. The tumor tissues fixed in 4% paraformaldehyde (at room temperature for 24 h) were embedded in paraffin and then sectioned into 5-$\mu$m-thick slices. Immunohistochemistry was performed using an Instant SABC-POD kit (cat. no. SA1020, Boster Biological Technology) according to the manufacturer's instructions. Briefly, after dewaxing, rehydration and antigen retrieval, the tumor sections were blocked and were then separately incubated with primary antibodies against pan-cytokeratin (AE1/AE3; cat. no. ab27988, Abcam, dilution: 1:200) and CPT1A (cat. no. ab128568, Abcam, dilution: 1:200) overnight at 4˚C. After washing, the sections were incubated with biotin-conjugated secondary antibody (cat. no. SA1020, Boster Biological Technology) at 37˚C for 30 min. After washing, the sections were incubated with SAB at 37˚C for 30 min and stained with DAB (cat. no. AR1027, Boster Biological Technology) at room temperature for 5 min. Following DAB visualization, the sections were immersed into water and then re-stained using hematoxylin at room temperature for 3 min. The AE1/AE3-positive cells or the CPT1A-positive cells were finally observed under a light microscope (Nikon Corporation).

*RNA immunoprecipitation (RIP) assay*. Anti-Argonaute 2 (AGO2) (cat. no. C34C6, Cell Signaling Technology, Inc.) and anti-IgG antibodies (cat. no. 8726S Cell Signaling Technology,

Inc.) were incubated with protein A+G beads at 4˚C for 1 h following the instructions provided with the RNA Immunoprecipitation kit (cat. no. P0101, Geneseed Biotech Co., Ltd.). Briefly, 1 ml Buffer A working solution contained 1% volume protease inhibitor and 1% volume RNase inhibitor before use. A total of $1x10^7$ GC-MSCs cells were used for each IP reaction and added 1 ml of the configured RIP lysis buffer. The lysate was centrifuged at 14,000 x g for 10 min, at 4˚C. The resulting supernatant and antibody-attached magnetic beads were incubated for 1 h at 4˚C. The product was obtained by centrifugation at 12,000 x g for 1 min at 4˚C. The captured RNAs and target protein were finally eluted and purified for RT-qPCR and western blot analyses.

*Luciferase reporter assay*. Wild-type or mutant circ_0024107 fragments were amplified by PCR and inserted into the luciferase reporter vector, GV272, provided by GeneChem. Wild-type or mutant 3'-untranslated region (3'UTR) CPT1A fragments were synthesized, annealed and inserted into the pmirGLO Dual-Luciferase miRNA Target Expression Vector (Promega Corporation). A total of 2 $\mu$g of the dual-luciferase gene vectors were co-transfected with 50 nM miRNA mimics into 293T cells (National Collection of Authenticated Cells Cultures) using Lipofectamine 2000®. After 5 h, cell culture media was refreshed. Cells were harvested for luciferase activity assay using a Dual-Luciferase Reporter Assay System (Promega Corporation) after transfection for 24 h. Luciferase activity was normalized to that of *Renilla* luciferase activity.

*gDNA extraction and amplification using PCR and agarose gel electrophoresis*. Genomic DNA small volume extraction kit (cat. no. D0063, Shanghai Biyuntian Biotechnology Co., Ltd.) was used to extract gDNA. The gDNA was then amplified by PCR. The 2% gel was prepared with 0.5X TAE. A total of 8 $\mu$l sample was added and 6 $\mu$l of 2,000 bp marker (Takara Bio, Inc.) at each end, and the voltage was set at 110 V for 30 min. Following electrophoresis, the gel was stained with 0.5 $\mu$g/ml ethidium bromide for 5 min, and imaged using an automatic gel imager (Biobase).

*Bioinformatics analysis*. Circ_0024107 annotation information was obtained using the circBase database (http://www.circbase.org). The Kyoto Encyclopedia of Genes and Genomes (KEGG) pathway database (https://www.kegg.jp/kegg/pathway.html) was used to analyze signaling pathway enrichment analysis. miRanda (http://www.microrna.org) and TargetScan (http://www.targetscan.org/) were used to predict potential binding miRNAs connecting circ_0024107 to CPT1A. Kaplan-Meier Plotter database (http://kmplot.com/) was used to assess the association between CPT1A, miR-5572 and miR-6855-5p and the survival of patients based on MSC abundance in gastric cancer tissues

*Statistical analysis*. SPSS software 22.0 and GraphPad Prism software 8.0 were used for statistical analyses. The data are expressed as the mean, mean ± SD, mean ± SEM, or median ± QR, as indicated in the figure legends. Statistically significant differences between parametric variables were calculated using an unpaired Student's t-test or one-way ANOVA followed by Tukey's post-hoc test, and non-parametric variables were analyzed using the Wilcoxon matched-pairs signed rank test was conducted to compare the expression of circ_0024107, miR-5572, miR-6855 and CPT1A between paired cancer tissues and adjacent non-cancerous tissues. The Chi-squared test was applied to analyze clinical significance between ordinal variables. The correlation of gene expression was examined using Spearman's correlation analysis. The Kaplan-Meier method and log rank test were used to evaluate the survival. A value of $P<0.05$ was considered to indicate a statistically significant difference.

## Results

*Screening and identification of GC-MSC-derived circ_0024107*. Previous studies by the authors have demonstrated that BM-MSCs are the critical cellular origin of GC-MSCs (6,16). In the present study, to identify deregulated circRNAs in GC-MSCs, a circRNA array was used to screen for differentially expressed circRNAs between GC-MSCs and BM-MSCs. A total of 5,497 circRNAs with a fold change ≥2 and $P<0.05$ were identified, including 2,545 upregulated and 2,952 downregulated circRNAs in the GC-MSCs (Fig. 1A and Table SIII). The top 10 upregulated circRNAs were selected for further verification using RT-qPCR (Fig. 1B); a consistently increased expression of hsa_circ_0024107 was observed in GC-MSCs (Fig. 1C). According to the annotation from the circBase database hsa_circ_002417 is generated from the host gene MMP1, being composed of exons 6-10 and having a length of 1,131 nucleotides. The amplified PCR products sequencing results verified the existence of back-splicing site (Fig. 1D). Furthermore, gDNA and cDNA were obtained from GC-MSCs and convergent primers and divergent primers were used to perform PCR. The electrophoresis results revealed that circ_0024107 was only amplified by divergent primers from the cDNA, not from gDNA (Fig. 1E). RNase R treatment confirmed that circ_0024107 was more stable than linear transcript MMP1 and β-actin (Fig. 1F). Subcellular fractionation assay verified that circ_0024107 was mainly located in the cytoplasm of the GC-MSCs (Fig. 1G). The aforementioned data indicate the successful identification and characterization of GC-MSC-derived circ_0024107.

*circ_0024107 is pivotal for GC-MSCs to promote gastric cancer cell metastasis in vitro and in vivo*. To determine the role of circ_0024107 in GC-MSCs, two siRNAs targeting back-splicing sites were synthesized and transfected into the GC-MSCs to knock down circ_0024107 (Fig. 2A and B). CM from the siRNA-transfected GC-MSCs was prepared and used for the culture of the AGS and HGC-27gastric cancer cells. *In vitro*, Transwell assays revealed that the knockdown of circ_0024017 markedly suppressed the GC-MSC-mediated stimulation of gastric cancer cell migration and invasion (Fig. 2C-E). In addition, circ_0024107-overexpressing plasmid was transfected into BM-MSCs to overexpress circ_0024107 (Fig. 2F and G). Notably, circ_0024107 conferred migration- and invasion-promoting roles to the BM-MSCs (Fig. 2H and I). *In vivo*, models of lymph node metastasis were established by inoculating HGC-27 cells

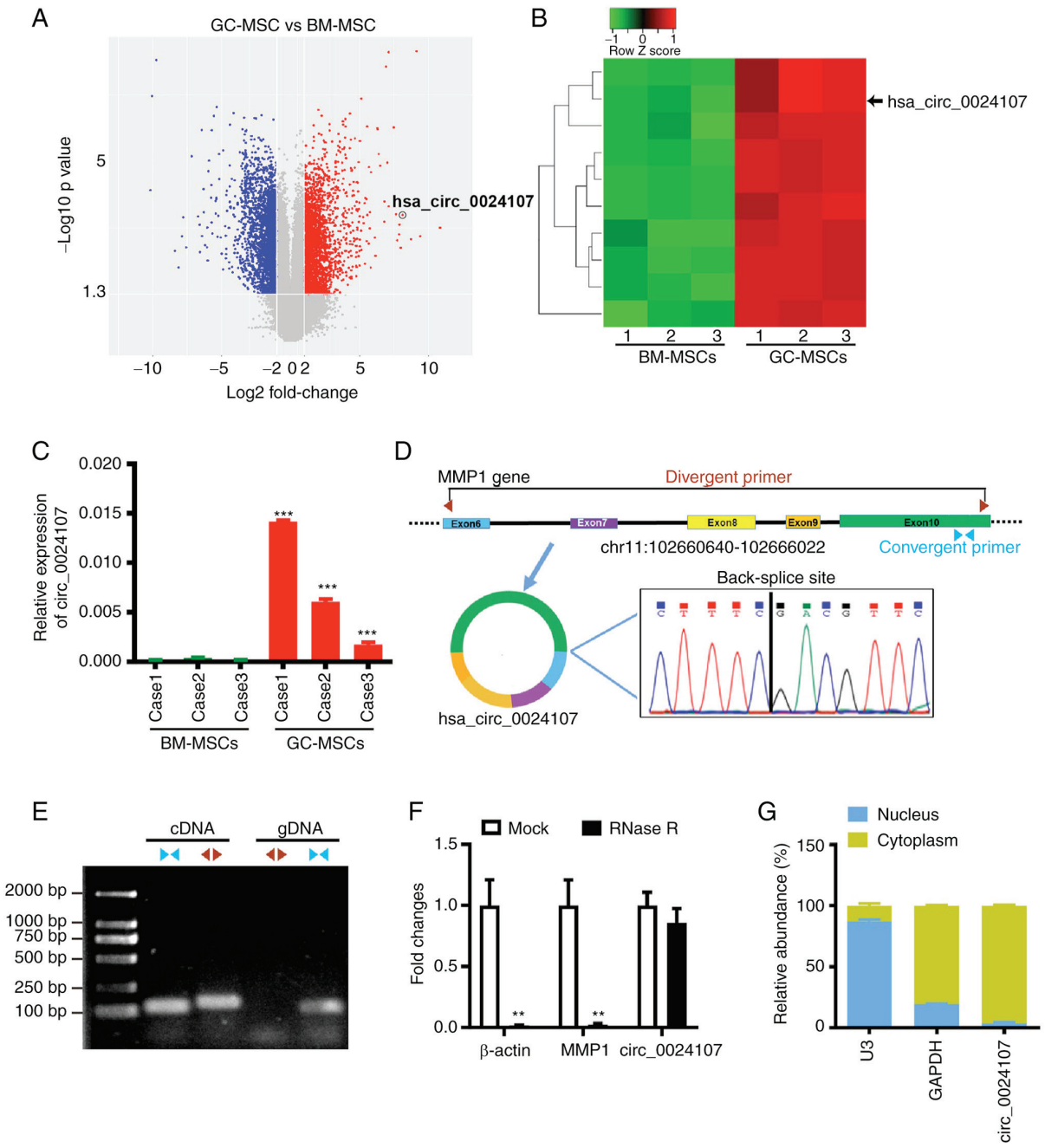


Figure 1. Screening and characterization of GC-MSC-derived circ_0024107. (A) Volcano plot of differently expressed circRNAs with fold changes ≥2 and P-values <0.05 between GC-MSCs and BM-MSCs. The circled dot indicates circ_0024107. (B) Heatmap illustrating the top 10 upregulated circRNAs in GC-MSCs vs. BM-MSCs. (C) RT-qPCR verification of microarray results in GC-MSCs and BM-MSCs from 3 cases of gastric cancer. (D) Schematic diagram of the genomic location and splicing mode of circ_0024107. The back-splice junction of circ_0024107 was analyzed by sanger sequencing. (E) cDNA and gDNA isolated from GC-MSCs were amplified with convergent and divergent primers. (F) RT-qPCR analysis of circ_0024107 and its linear host gene, MMP1, in GC-MSCs treated with RNase R. β-actin was used as the negative control. (G) Subcellular localization of circ_0024107 assay. Values are presented as the mean ± SD (n=3). $^{**}$P<0.01 and $^{***}$P<0.001, vs. BM-MSCs. circRNA, circular RNA; GC-MSCs, gastric cancer-derived mesenchymal stem cells; BM-MSCs, bone marrow-derived mesenchymal stem cells; RT-qPCR, reverse transcription-quantitative PCR.

treated with different GC-MSC-CM into the left footpads of nude mice. The reduced volume and weight of popliteal lymph nodes and inguinal lymph nodes were observed, as well as a smaller positive expression area of pan-cytokeratin AE1/AE3 in the lymph node tissues in the si-circ_0024107-transfected groups compared with those in the negative control-transfected groups (Fig. 2K-M). These findings suggest that circ_002417 is crucial for the promoting effects of GC-MSCs on gastric cancer cell metastasis.

*GC-MSCs undergo fatty acid oxidation (FAO) metabolic reprogramming to exert tumor-promoting regulatory effects.* To investigate whether GC-MSCs undergo metabolic reprograming, a cDNA array was applied to screen differentially expressed mRNAs between the GC-MSCs and BM-MSCs. Compared to the BM-MSCs, a total of 2,276 differentially expressed mRNAs (1,162 upregulated and 1,114 downregulated) were identified in the GC-MSCs based on the same criteria for circRNA screening (Fig. 3A and Table SIV).

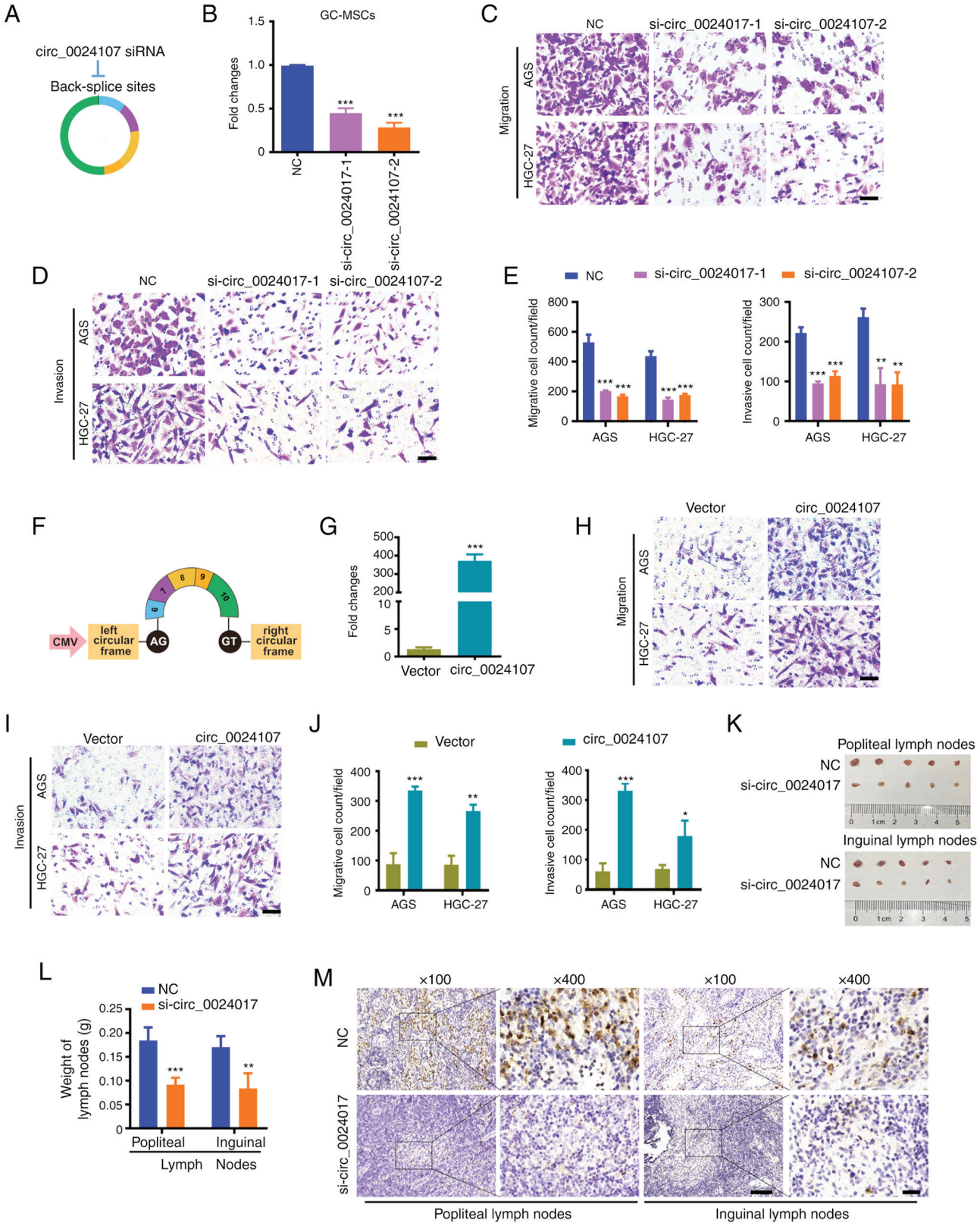


Figure 2. circ_0024107 mediates the promotion of gastric cancer cell metastasis by GC-MSCs *in vitro* and *in vivo*. (A) Schematic diagram of the specific siRNAs targeting the back-splicing site of circ_0024107. (B) RT-qPCR of circ_0024107 in GC-MSCs following transfection with two different siRNAs against circ_0024107. NC was the negative control of the two siRNAs. (C-E) Transwell assays of the migration and invasion of gastric cancer cell lines, AGS and HGC-27, following treatment with CM from circ_0024107-silencing GC-MSCs. Scale bars, 100 $\mu$M; magnification, x200. (F) Schematic diagram of circ_0024107 overexpression vector. (G) RT-qPCR of circ_0024107 in BM-MSCs following transfection with the overexpression vector. (H-J) Migration and invasion analysis of gastric cancer cells following treatment with CM from circ_0024107-overexpressing BM-MSCs. Scale bars, 100 $\mu$M; magnification, x200. (K-M) Lymphatic metastasis of HGC-27 treated with CM from circ_0024107-silenced GC-MSCs *in vivo*. (K) Lymph nodes; (L) weight of lymph nodes; (M) representative images of pan-cytokeratin AE1/AE3 staining in lymph nodes. Magnification, x100 and scale bars, 100 $\mu$M; or magnification, x400 and scale bars, 20 $\mu$M. Values are presented as the mean ± SD (n=3) $^{*}$P<0.05, $^{**}$P<0.01 and $^{***}$P<0.001, vs. respective control. circRNA, circular RNA; GC-MSCs, gastric cancer-derived mesenchymal stem cells; BM-MSCs, bone marrow-derived mesenchymal stem cells; RT-qPCR, reverse transcription-quantitative PCR; CM, conditioned medium.

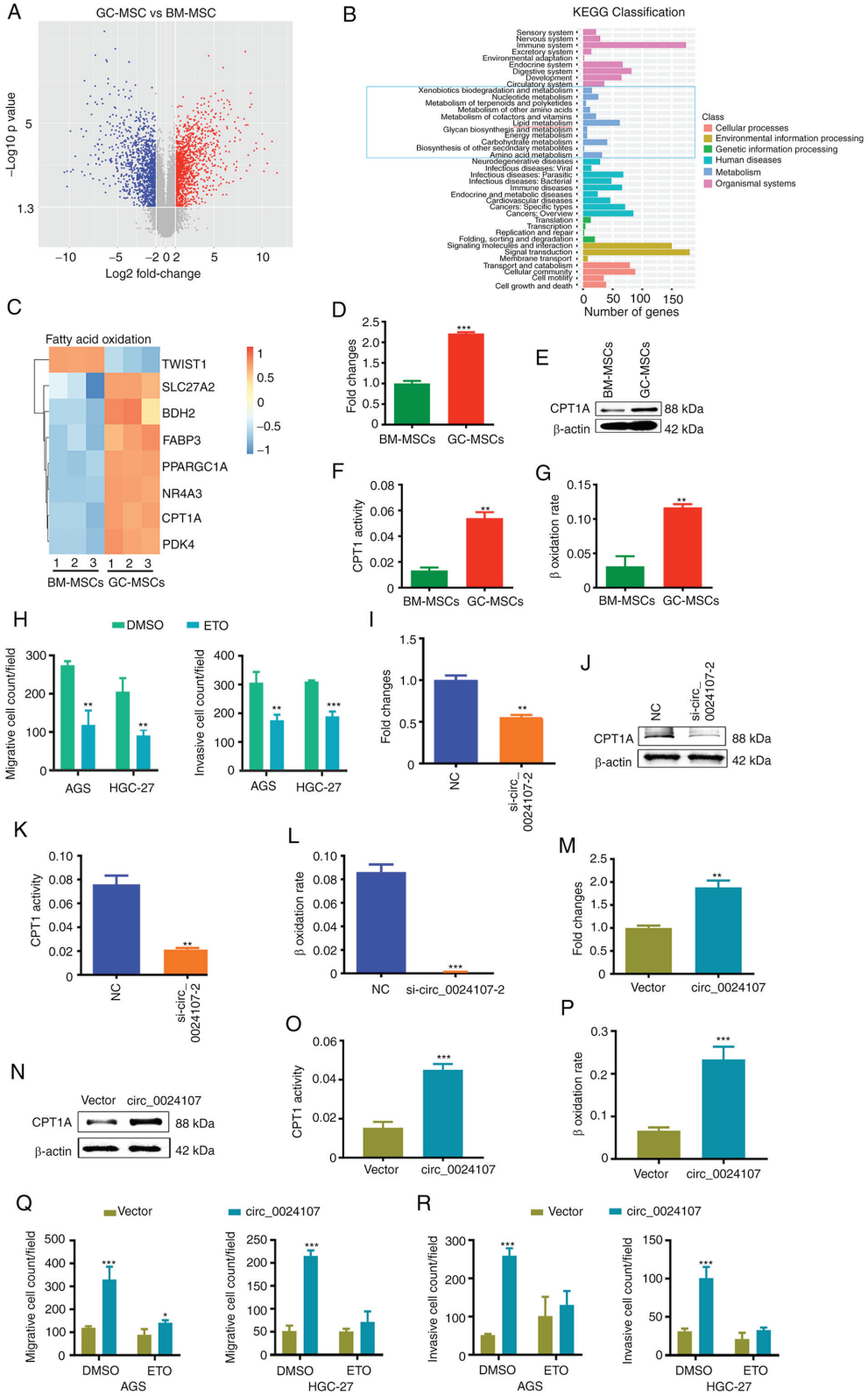


Figure 3. FAO reprogramming is crucial for the oncogenic role of GC-MSCs and circ_0024107 modulates the FAO metabolic reprogramming of GC-MSCs by upregulating CPT1A expression. (A) Volcano plot of differentially expressed mRNAs with fold changes ≥2 and P-values <0.05 between GC-MSCs and BM-MSCs. (B) KEGG classification analysis of the deregulated mRNAs; the blue bars in the light blue box are related to metabolism; (C) Heatmap of different genes involved in FAO metabolism. (D) RT-qPCR verification of CPT1A mRNA levels in GC-MSCs and BM-MSCs. (E) Western blot analysis of CPT1A protein levels in the two types of MSCs. (F,G) FAO activity was compared between GC-MSCs and BM-MSCs by (F) CPT1 activity assay and (G) β-oxidation rate detection. (H) Count of the migrated and invaded gastric cancer cells following incubation with CM from etomoxir-treated GC-MSCs. (I-L) The effects of circ_0024107 silencing on (I) CPT1A mRNA levels, (J) protein levels, (K) CPT1 activity and (L) β-oxidation rate in GC-MSCs. (M-P) The effects of circ_0024107 overexpression on (M) CPT1A mRNA levels, (N) protein levels, (O) CPT1 activity and (P) β-oxidation rate in BM-MSCs. (Q,R) Count of (Q) migrated and (R) invaded gastric cancer cells following culture with CM from circ_0024107-overexpressing BM-MSCs treated with etomoxir. Values are presented as the mean ± SD (n=3). $^{*}$P<0.05, $^{**}$P<0.01 and $^{***}$P<0.001, vs. respective control. circRNA, circular RNA; GC-MSCs, gastric cancer-derived mesenchymal stem cells; BM-MSCs, bone marrow-derived mesenchymal stem cells; RT-qPCR, reverse transcription-quantitative PCR; CM, conditioned medium; CPT1A, carnitine palmitoyltransferase 1A; FAO, fatty acid oxidation; ETO, etomoxir.

KEGG pathway enrichment analysis revealed that lipid metabolism was dominant in the metabolism module (Fig. 3B). Recent research has suggested that FAO emerges as a critical aspect of the metabolic landscape of cancer (18). Heatmap analysis revealed that the majority of genes driving FAO metabolism were upregulated in the GC-MSCs, including the limiting enzyme, CPT1A (Fig. 3C). CPT1A mRNA and protein levels were verified to be increased in the GC-MSCs relative to those in the BM-MSCs (Fig. 3D and E). CPT1 activity and β-oxidation rate assays confirmed that FAO was highly activated in the GC-MSCs compared to the BM-MSCs (Fig. 3F and G). In order to clarify whether FAO mediates the oncogenic function of GC-MSCs, etomoxir (CPT1A inhibitor) was used to block FAO in GC-MSCs. As demonstrated by the results, the stimulated invasion of the gastric cancer cells by GC-MSCs was significantly attenuated by treatment with etomoxir (Figs. 3H and S1A). These findings indicate that FAO metabolic reprogramming is crucial for the oncogenic function of GC-MSCs.

*circ_0024107 increases FAO activity in GC-MSCs by upregulating CPT1A expression*. The aforementioned findings suggested that circ_0024107 and FAO are critical for GC-MSC function. The present study then wished to determine whether there is a regulatory association between them. Cells in which circ_0024107 was knocked down or overexpressed were separately subjected to CPT1A expression and FAO activity analyses. The CPT1A mRNA and protein expression levels were consistently altered along with the knockdown or overexpression of circ_0024107 in MSCs (Fig. 3I, J, M and N). CPT1 activity and β-oxidation rate were suppressed in the circ_0024107-silenced GC-MSCs, whereas they were increased in the circ_0024107-overexpressing BM-MSCs (Fig. 3K, L, O and P). Furthermore, pre-treatment with etomoxir notably impaired the effects of circ_0024107 overexpression in BM-MSCs on gastric cancer cell invasion (Figs. 3Q and R, and S1B). In summary, circ_0024107-induced FAO metabolic reprogramming is crucial for the oncogenic function of GC-MSCs.

*circ_0024107 acts as a sponge of miR-5572 and miR-6855-5p to upregulate CPT1A expression*. To evaluate whether circ_0024107 induced FAO by acting as a miRNA sponge to upregulate CPT1A expression, miRanda and TargetScan were used to predict potential binding miRNAs connecting circ_0024107 to CPT1A. The overlapped hsa_miR-5572 and hsa_miR-6855-5p were eventually selected as candidate miRNAs for subsequent analyses (Fig. 4A). circ_0024107-luciferase reporter vectors containing the wild-type or mutant binding sequences were constructed (Fig. 4B) and co-transfected with miRNA mimics. The luciferase activity of the wild-type vectors was evidently reduced by miRNA mimics compared to that of miRNA mimics negative control (MNC). No marked differences were observed for the mutant-type vectors (Fig. 4C). Moreover, the results of RIP assay revealed that circ_0024107 and the two miRNAs were pulled down by anti-AGO2 compared with control IgG (Fig. 4D). The miR-5572 and miR-6855-5p levels were markedly increased in the circ_0024107-silenced GC-MSCs, whereas they were reduced in the circ_0024107-overexpressing BM-MSCs (Fig. 4E and F). These data illustrate that circ_0024107 physically interacts with and negatively regulates miR-5572 and miR-6855-5p.

To examine whether CPT1A is the target of miR-5572 and miR-6855-5p, dual-luciferase reporter plasmids containing the wild-type or mutant CPT1A 3'UTR fragments were separately constructed according to the prediction sites for the two miRNAs (Fig. 4G). Both miR-5572 and miR-6855-5p mimics notably suppressed the luciferase activities of the wild-type plasmids, but not those of the mutant types (Fig. 4H). The overexpression of miR-5572 and miR-6855-5p in GC-MSCs following mimic transfection resulted in reduced CPT1A mRNA and protein levels (Fig. 4I and K). Conversely, the reduced expression of the two miRNAs in the BM-MSCs following inhibitor transfection increased CPT1A expression (Fig. 4J and L). These results indicate that miR-5572 and miR-6855-5p negatively regulate CPT1A mRNA by binding to its 3'UTR.

*miR-5572 and miR-6855-5p reverse the circ_0024107-induced FAO metabolic reprogramming of GC-MSCs*. Based on the aforementioned findings, it was hypothesized that the two miRNAs may suppress FAO and attenuate the oncogenic role of GC-MSCs. The corresponding miRNA mimics and inhibitors were utilized to overexpress and suppress the two miRNAs in the GC-MSCs and BM-MSCs, respectively. FAO activity was negatively associated with the levels of both miRNAs (Fig. 5A-D). The pro-invasive role of the GC-MSCs was attenuated by miRNA mimics, whereas the tumor-promoting role was conferred to the BM-MSCs by miRNA inhibitors (Figs. 5E and F, and S2A and B). Furthermore, treatment with etomoxir significantly reversed the effects induced by the BM-MSCs transfected with miRNA inhibitors (Figs. 5G and S2C). To further elucidate whether circ_0024107 functions as a competitive endogenous RNA (ceRNA) to upregulate CPT1A, the circ_0024107 overexpression vector was separately co-transfected with the two miRNA mimics into BM-MSCs. The CPT1A mRNA and protein levels induced by circ_0024107 overexpression were significantly reversed by transfection with miRNA mimics (Fig. 5H and I). A similar tendency was observed for CPT1 activity and β-oxidation rate (Fig. 5J and K). In addition, the promotion of gastric cancer cell migration and invasion induced by circ_0024107-overexpressing BM-MSCs was eliminated by the two miRNA mimics (Fig. 5L and M). These data thus indicate that circ_0024107 elicits the FAO reprograming of GC-MSCs by sponging miR-5572 and miR-6855-5p.

*GC-MSC-derived circ_0024107 modulates FAO in gastric cancer cells*. A previous study by the authors demonstrated that increased FAO levels are indispensable for lymphatic metastatic gastric cancer cells (19). GC-MSCs possibly promote lymphatic metastasis by inducing FAO of gastric cancer cells. In the present study, as was expected, the HGC-27 cells cultured with GC-MSC-CM exhibited higher levels of CPT1 activity and β-oxidation rate than those incubated with BM-MSC-CM (Fig. 6A and B). Pre-treatment with etomoxir eliminated the promoting effects of GC-MSCs on gastric cancer cell migration and invasion (Fig. 6C and D). The results of RT-qPCR verified that the circ_0024017

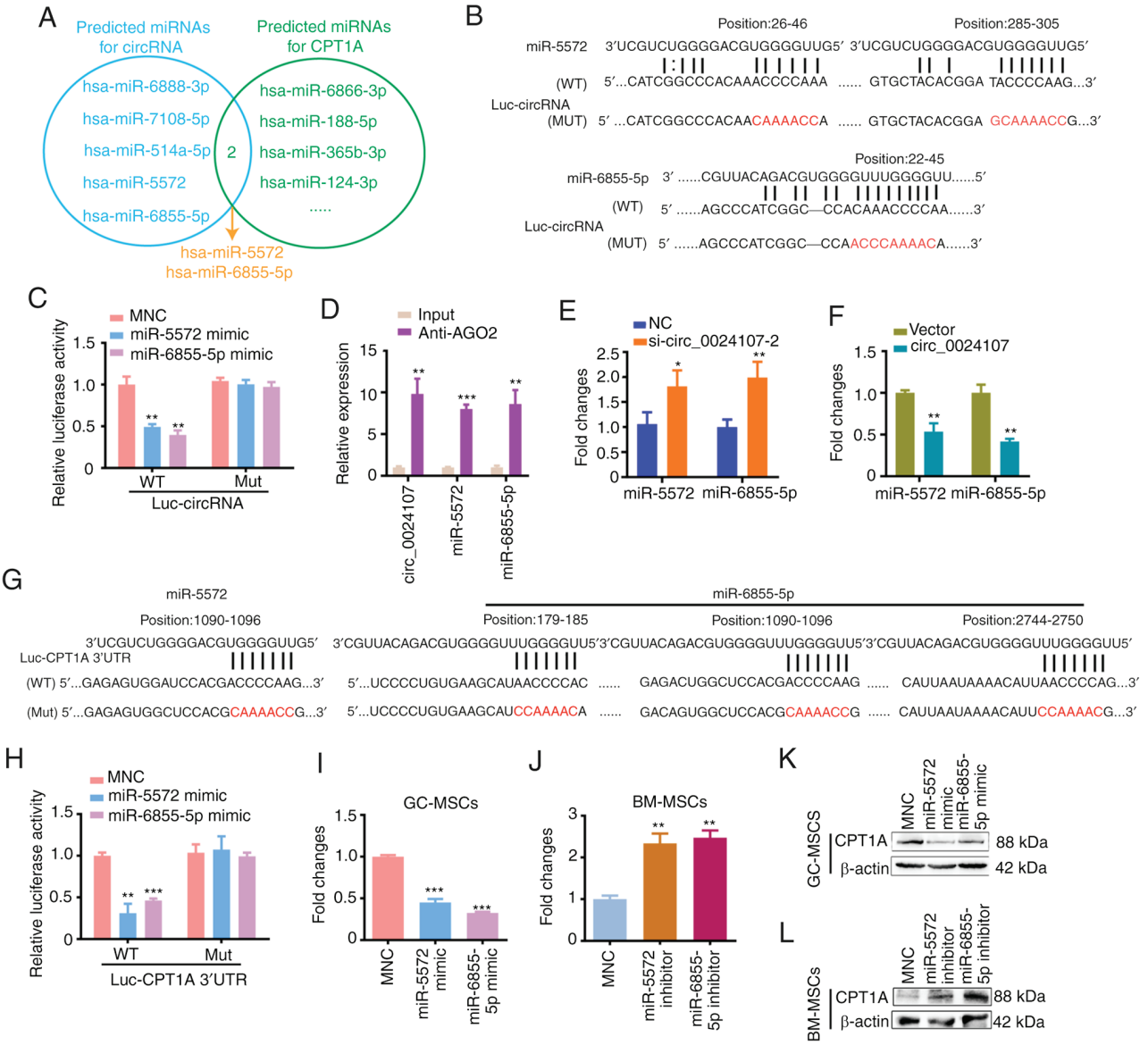


Figure 4. circ_0024107 upregulates CPT1A expression by sponging miR-5572 and miR-6855-5p. (A) Overlapped miRNAs analysis between the predicted downstream miRNAs sponging by circ_0024107 and the potential miRNAs target regulating CPT1A, predicted using miRanda and TargetScan. (B) circ_0024107-WT and circ_0024107-Mut luciferase reporter construction based on the predicted miRNA binding sites. (C) Luciferase activity assay following the co-transfection of luciferase reporters with miRNA mimics. (D) RIP assay was performed using the anti-AGO2 antibody in GC-MSCs. (E and F) RT-qPCR of the two miRNA levels in (E) circ_0024107-silenced GC-MSCs and (F) circ_0024107-overexpressing BM-MSCs. (G) CPT1A 3'UTR-WT and CPT1A 3'UTR-Mut luciferase reporter construction based on the predicted miRNA binding sites. (H) Luciferase activity assay. (I-L) RT-qPCR and western blot analysis of CPT1A levels in (I and K) miRNA mimic-transfected GC-MSCs and (J and L) inhibitor-transfected BM-MSCs. Values are presented as the mean ± SD (n=3). $^{*}$P<0.05, $^{**}$P<0.01 and $^{***}$P<0.001, vs. respective control. circRNA, circular RNA; GC-MSCs, gastric cancer-derived mesenchymal stem cells; BM-MSCs, bone marrow-derived mesenchymal stem cells; RT-qPCR, reverse transcription-quantitative PCR; CPT1A, carnitine palmitoyltransferase 1A.

and CPT1A levels were notably increased, while those of miR-5572 and miR-6855-5p were reduced in the HGC-27 cells treated with GC-MSC-CM (Fig. 6E and F). circ_0024107 silencing in HGC-27 cells not only suppressed the migrative and invasive capacities and FAO activity, but also blocked the effects of GC-MSCs on cell migration, invasion and FAO (Figs. 6G-J and S3A-G). The miR-5572 and miR-6855-5p expression levels were negatively associated with the circ_0024107 and CPT1A levels in circ_0024107-silenced HGC-27 cells (Figs. 6K and L and S3H). The overexpression of the two miRNAs not only significantly suppressed CPT1A expression at the mRNA and protein level, but also inhibited HGC-27 cell migration and invasion (Fig. S4). Moreover, the knockdown of circ_0024017 in the GC-MSCs markedly weakened their effects on inducing circRNA and CPT1A expression, enhancing FAO activity and suppressing miRNAs in the HGC-27 cells (Fig. 6M-P). On the whole, these data suggest that circ_0024107 mediates the crosstalk between GC-MSCs and gastric cancer cells, and may synergistically promote gastric cancer lymphatic metastasis.

*Expression profiles and clinical implications of the circ_0024107/miR-5572/6855-5p/CPT1A axis in gastric cancer.* RT-qPCR analysis revealed that the circ_0024107 and CPT1A levels were aberrantly increased, whereas the levels of the two miRNAs were significantly decreased in

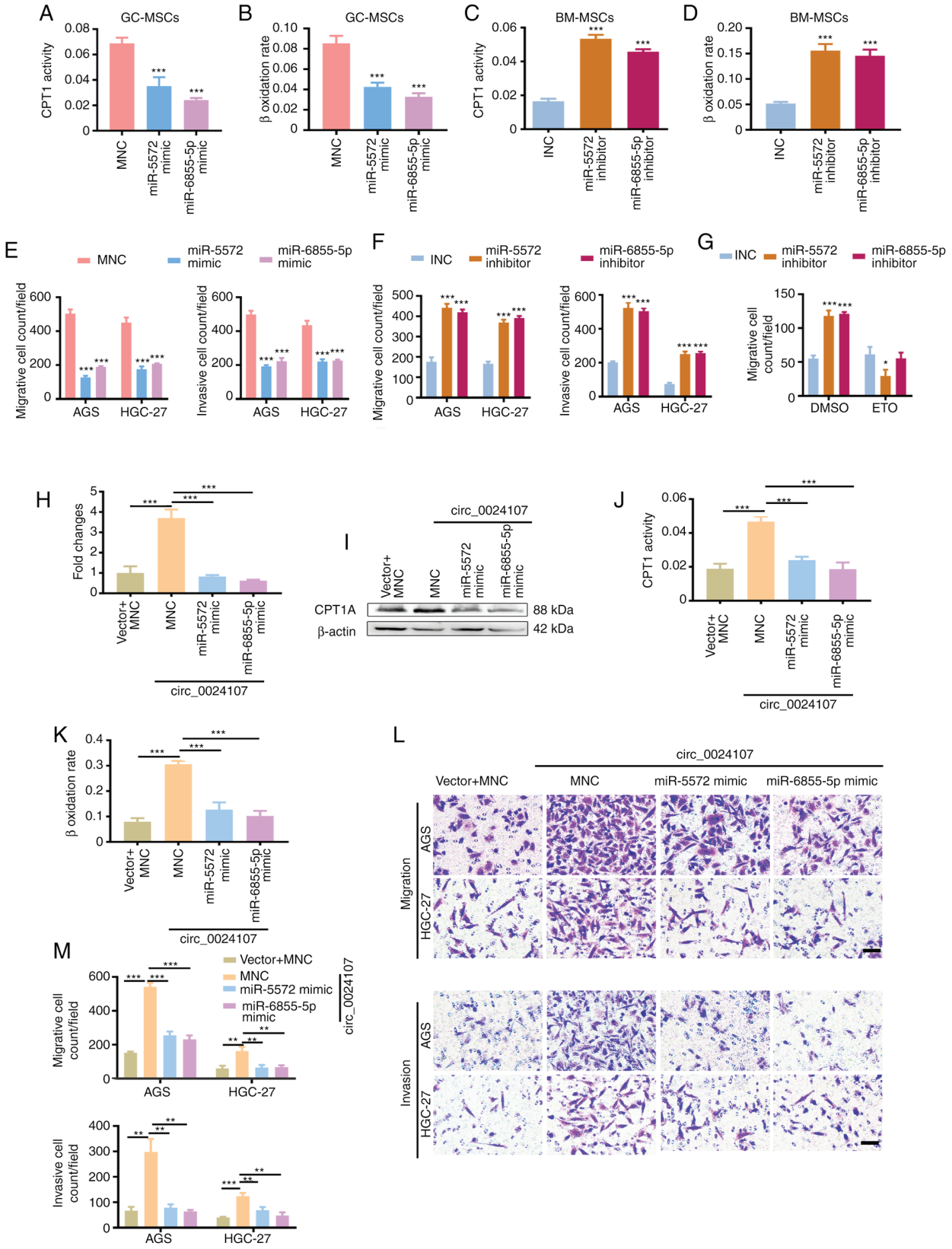


Figure 5. miR-5572 and miR-6855-5p reverse the circ_0024107-induced FAO reprograming of GC-MSCs. (A-D) CPT1 activity and β-oxidation rate assay in (A and B) miRNA mimic-transfected GC-MSCs and (C and D) inhibitor-transfected BM-MSCs. (E and F) Count of the migrated and invaded gastric cancer cells following incubation with CM from (E) miRNA mimic-transfected GC-MSCs and (F) inhibitor-transfected BM-MSCs. (G) Count of the migrated gastric cancer cells following incubation with CM from BM-MSCs in which the two miRNAs were silenced and which were treated with etomoxir. Detection of (H) CPT1A mRNA and (I) protein levels in BM-MSCs co-transfected with circ_0024107 overexpression vector and miRNA mimics. Measurement of FAO activity assay by determining (J) CPT1 activity and (K) β-oxidation rate in the co-transfected BM-MSCs. (L and M) Transwell assay of the migration and invasion of gastric cancer cells following incubation with CM from the co-transfected BM-MSCs. Scale bars, 100 $\mu$M; magnification, x200. Values are presented as the mean ± SD (n=3). $^{*}$P<0.05, $^{**}$P<0.01 and $^{***}$P<0.001, vs. respective control. circRNA, circular RNA; GC-MSCs, gastric cancer-derived mesenchymal stem cells; BM-MSCs, bone marrow-derived mesenchymal stem cells; CPT1A, carnitine palmitoyltransferase 1A; CM, conditioned medium; FAO, fatty acid oxidation; ETO, etomoxir.

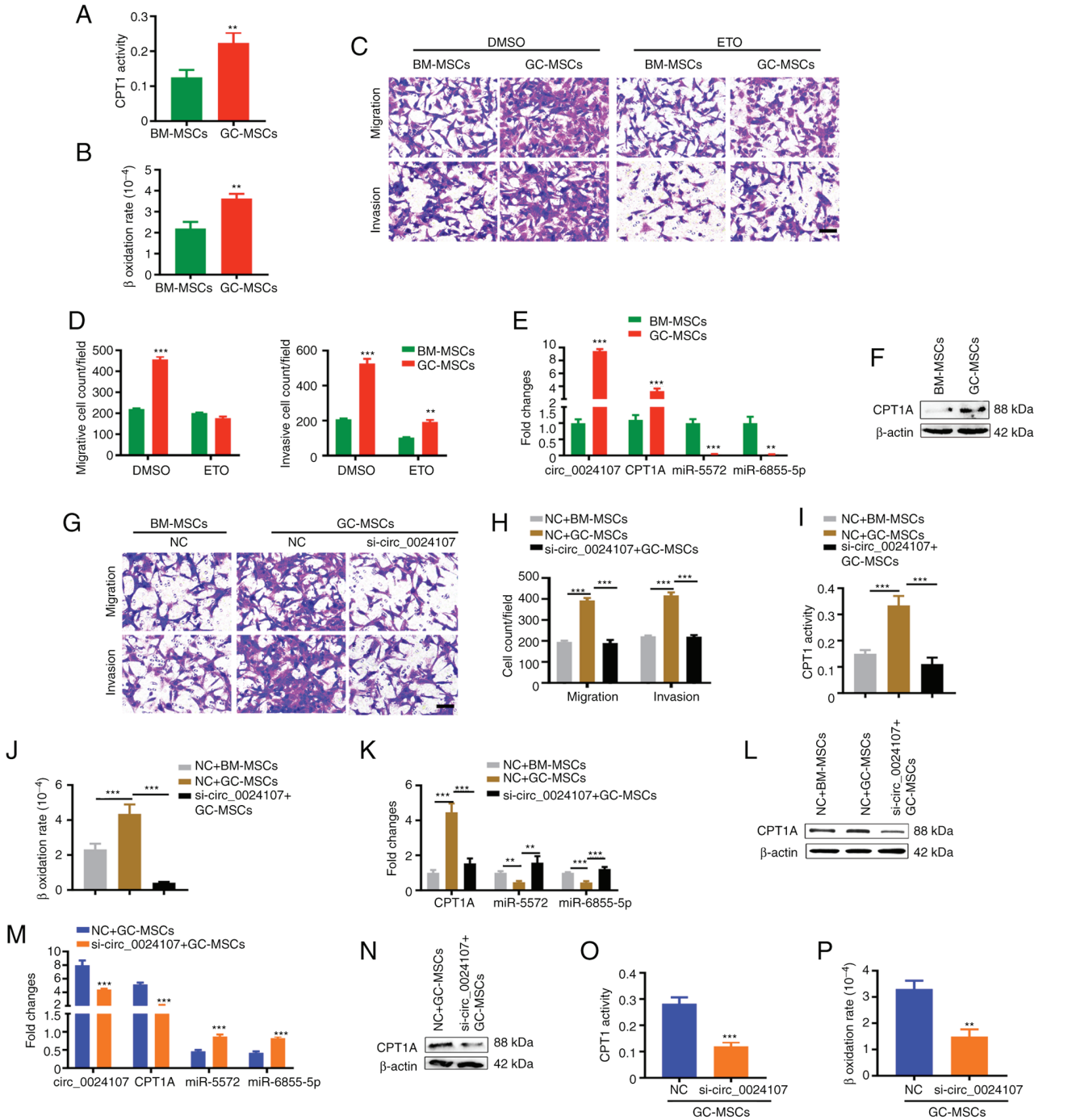


Figure 6. GC-MSCs promote metastasis by modulating the circ_0024107/miR-5572/6855-5p/CPT1A axis in gastric cancer cells. (A) CPT1 activity and (B) β-oxidation rate detection in HGC-27 cells following treatment with GC-MSC-CM and BM-MSC-CM. (C and D) Migration and invasion of HGC-27 cells pre-treated with etomoxir and incubated with MSC-CM. (E and F) Comparison of circ_0024107, CPT1A, miR-5572 and miR-6855-5p levels in HGC-27 cells following treatment with GC-MSC-CM and BM-MSC-CM using (E) reverse transcription-quantitative PCR and (F) western blot analysis. (G and H) Migration and invasion of circ_0024107-silenced HGC-27 cells following incubation with GC-MSC-CM. (I and J) FAO activity of circ_0024107-silenced HGC-27 cells following incubation with GC-MSC-CM. (K) Detection of CPT1A, miR-5572 and miR-6855-5p levels, and (L) CPT1A protein content in circ_0024107-silenced HGC-27 cells treated with GC-MSC-CM. (M) Detection of circ_0024107, CPT1A, miR-5572 and miR-6855-5p levels, and (N) CPT1A protein content in HGC-27 cells following incubation with the CM from circ_0024107-silenced GC-MSCs. (O and P) FAO activity of HGC-27 cells following incubation with the CM from circ_0024107-silenced GC-MSCs. Scale bars, 100 $\mu$M; magnification, x200. Values are presented as the mean ± SD (n=3). $^{**}$P<0.01 and $^{***}$P<0.001. circRNA, circular RNA; GC-MSCs, gastric cancer-derived mesenchymal stem cells; BM-MSCs, bone marrow-derived mesenchymal stem cells; CPT1A, carnitine palmitoyltransferase 1A; CM, conditioned medium; FAO, fatty acid oxidation; ETO, etomoxir.

cancer tissues compared to paired adjacent normal tissues (Fig. 7A). The circ_0024107 expression levels positively correlated with the CPT1A levels, whereas the miR-5572 and miR-6855-5p levels negatively correlated with the CPT1A levels (Fig. 7B-D). A significant negative correlation was detected between circ_0024107 and miR-5572; however, the correlation between circ_0024107 and miR-6855-5p was not significant (Fig. 7E and F). The circ_0024107 level

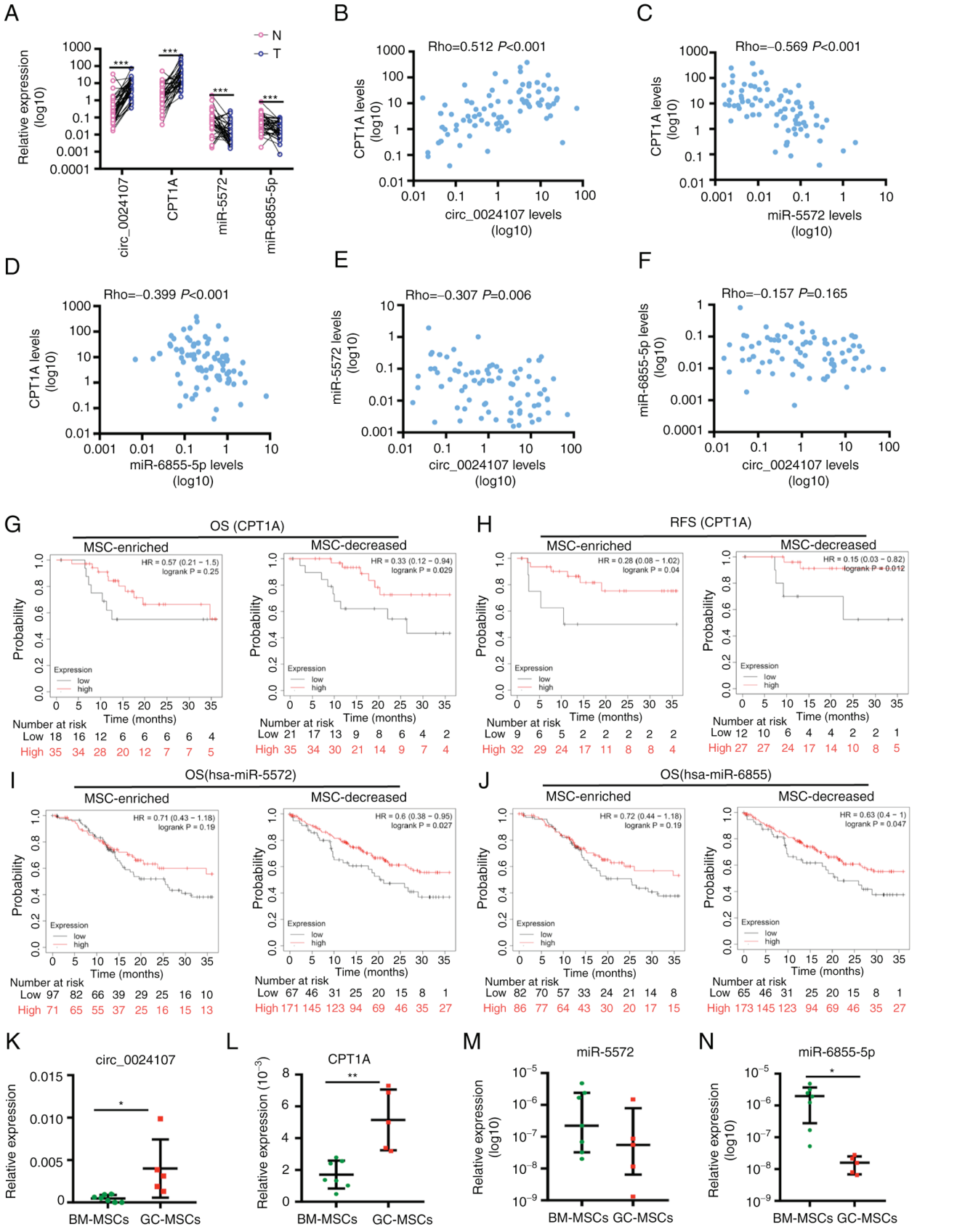


Figure 7. Expression profiles and clinical implications of the circ_0024107/miR-5572/6855-5p/CPT1A axis in gastric cancer. (A) Comparison of circ_0024107, CPT1A, miR-5572 and miR-6855-5p levels between 40 gastric cancer tissues (T) and paired adjacent gastric tissues (N). (B-F) Correlation analysis of molecules involved in this axis. (G-J) Survival analysis of (G and H) CPT1A, (I) miR-5572 and (J) miR-6855-5p in gastric cancer tissues with an MSC-enriched status or and with decreased numbers of MSCs using the Kaplan-Meier Plotter database. (K-N) Comparison of circ_0024107-miR-5572/6855-5p/CPT1A axis expression levels between GC-MSCs and BM-MSCs. (A-F) Values are presented as the mean (n=3); (K, L and N) Values are presented as mean ± SEM (n=3); (M) Values are presented as the median ± QR (n=3). $^{*}$P<0.05, $^{**}$P<0.01 and $^{***}$P<0.001, vs. respective control. circRNA, circular RNA; GC-MSCs, gastric cancer-derived mesenchymal stem cells; BM-MSCs, bone marrow-derived mesenchymal stem cells; CPT1A, carnitine palmitoyltransferase 1A; OS, overall survival; RFS, recurrence-free survival.

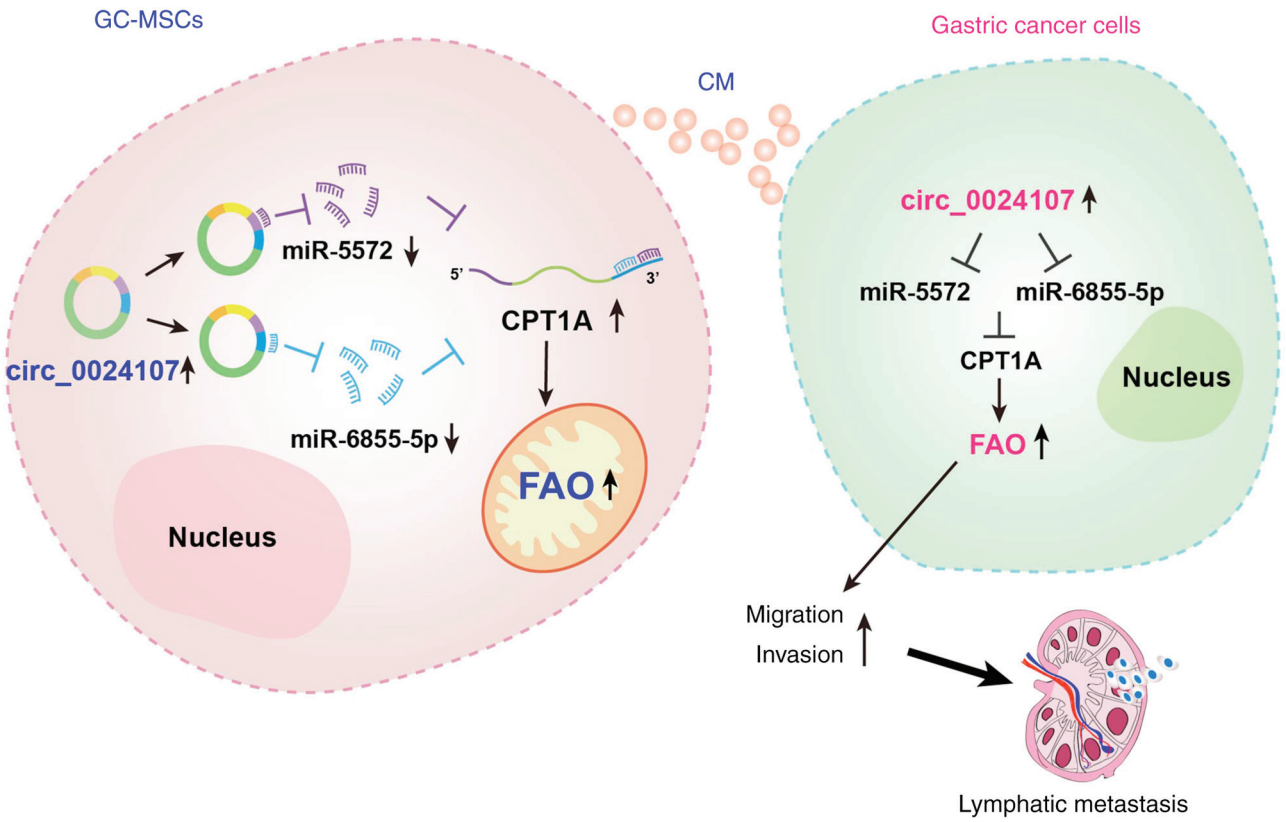


Figure 8. Schematic diagram of the mechanisms through which GC-MSC-derived circ_0024107 promotes gastric cancer cell lymphatic metastasis via FAO metabolic reprogramming mediated by the miR-5572/6855-5p/CPT1A axis. circRNA, circular RNA; GC-MSCs, gastric cancer-derived mesenchymal stem cells; CPT1A, carnitine palmitoyltransferase 1A; FAO, fatty acid oxidation.

was also found to be associated with lymph node metastasis status and TNM stage, whereas CPT1A was only associated with lymph node metastasis status. However, no association was observed between the two miRNAs and the clinical features of patients with gastric cancer (Table SV). The Kaplan-Meier Plotter database was used to assess the association between CPT1A, miR-5572 and miR-6855-5p and the survival of patients based on MSC abundance in gastric cancer tissues. Of note, CPT1A was a favorable factor, not only associated with 3-year OS of patients with stage II gastric cancer, whose cancer tissues contained decreased numbers of MSCs, but also with the 3-year recurrence-free survival of patients at the same stage, irrespective of the MSC enrichment status (Fig. 7G and H). The two miRNAs only served as favorable prognostic factors for patients with a MSC enrichment status (Fig. 7I and J). Furthermore, GC-MSCs another 5 patients and BM-MSCs from another 7 patients were randomly selected to evaluate the expression profile of the axis. Compared to the BM-MSCs, the circ_0024107 and CPT1A levels were markedly increased in the GC-MSCs, whereas the miR-6855-5p level was significantly decreased. By contrast, the miR-5572 levels were decreased in the GC-MSCs, although without a significant difference (Fig. 7K-N). In addition, a positive correlation was detected between circ_0024107 and CPT1A expression, while a negative correlation was only observed between miR-6855-5p and CPT1A, as well as between the miRNAs and circ_0024107 (Fig. S5). These results suggest that the regulatory axis is deregulated in gastric cancer tissues and GC-MSCs, and is associated with lymph node metastasis and prognosis of gastric cancer.

## Discussion

During the metastasis process and during chemoradiotherapy, cancer cells strive for survival, depending on interactions with surrounding stromal cells to overcome stressful conditions, such as nutrient deficiency (20). Cancer cells alter metabolic procedures to adapt to different environments, while stromal cells need to undergo metabolic reprogramming to release supportive signaling or provide necessary metabolites for cancer cell biosynthesis (21,22). Therefore, tumor stromal cells are a critical for the understanding of the mechanisms through which cancer evolves and for the development of an effective therapeutic strategy. The present study focused on gastric cancer-associated MSCs and revealed that GC-MSC-derived circ_0024107 promoted gastric cancer cell lymphatic metastasis via FAO metabolic reprogramming mediated by the miR-5572/6855-5p-CPT1A axis.

Lymph node metastasis is an independent poor prognostic predictor of gastric cancer. Over the past decades, an increasing number of tissue- and plasma-derived circRNAs have been demonstrated to be associated with the lymphatic metastasis of gastric cancer (23,24). CircRNAs are sometimes used to clarify the regulatory mechanisms of specific molecules involved in the lymph node metastasis of gastric cancer (25). A recent study determined circRNA profiles in cancer-associated fibroblasts (CAFs) and identified that CAF-specific

circCUL2 conferred the CAF phenotype on normal fibroblasts and mediated the CAF oncogenic effects by modulating the miR-203a-3p/MyD88/NF-κB/IL6 axis (26). Likewise, herein, it was proved that a large number of circRNAs were aberrantly expressed in GC-MSCs, and GC-MSC-derived circ_0024107 was found to be was pivotal for GC-MSCs to promote gastric cancer cell lymphatic metastasis. Ba *et al* (27) revealed that gastric cancer cell-derived exosomes probably promoted the migration and homing of adipose-derived MSCs by inducing their circRNA deregulation. These findings support the results of the present study, in that circRNAs are actually deregulated in gastric cancer-associated MSCs and may play multiple roles in gastric cancer progression. Furthermore, the alteration of circ_0024017 expression in gastric cancer cells upon GC-MSC-CM treatment and the knockdown of circ_0024107 in gastric cancer cells eliminated the tumor-promoting effects of GC-MSCs, which suggested that circ_0024107 mediates the crosstalk between GC-MSCs and gastric cancer cells to synergistically promote gastric cancer metastasis.

A previous study indicated that immune cells, such as regulatory $CD4^+$ T-cells (Tregs), M2 macrophages, myeloid-derived suppressor cells and dendritic cells relied on FAO to adopt immunosuppressive phenotypes to help cancer cell immune evasion (18). GC-MSCs are essentially immune cells. Consistently, the data from the present study verified that GC-MSCs acquired oncogenic functions, dependent on FAO metabolic reprogramming. A previous study by the authors confirmed that FAO was indispensable for gastric cancer cells to sustain a lymphatic metastatic capacity and its activity was increased along with the enhanced lymphatic metastatic capacity of gastric cancer cells (19). Recent studies have reported that MSCs induced FAO in gastric cancer cells to acquire stemness and chemoresistance (28,29), which supports the current findings that GC-MSCs promoted cancer cell migration and invasion by inducing FAO in gastric cancer cells. Compared to the findings of these two previous studies (28,29), the present study revealed a different mechanism regulated by GC-MSC-derived circRNA. These data further highlight the critical role of FAO metabolic reprogramming in stromal cells and cancer cells for malignant progression. The targeted blocking of FAO thus represents a promising alternative approach for cancer therapy.

It has been demonstrated that a large number of circRNAs are aberrantly expressed in almost all cancer types and have been shown to play indispensable roles in almost all aspects of cancer cell biological behavior, including metabolic reprogramming (30,31). However, only a limited number of studies have examined the mechanisms of fatty acid metabolism in cancer by the exploration of circRNAs (32,33). Herein, it was demonstrated that the FAO mediated by the circ_0024107-miR-5572/6855-5p-CPT1A axis not only conferred an oncogenic function on GC-MSCs, but was also involved in gastric cancer cells treated with GC-MSC-CM. Relative to the gastric cancer cells treated with BM-MSC-CM, higher levels of circ_0024107 in gastric cancer cells were induced after GC-MSC-CM treatment. Therefore, the knockdown of circ_0024107 hampered the oncogenic role of GC-MSCs attributed to the direct and indirect blocking of FAO reprogramming in GC-MSCs and gastric cancer cells, which at least provides an explanation for the unilateral intervention of circ_0024107 in GC-MSCs being sufficient to inhibit gastric cancer metastasis *in vivo*. However, further research is required in order to elucidate the mechanisms through which GC-MSC-CM affect the circ_0024107 levels in gastric cancer cells.

A previous study by the authors reported that CPT1A was an unfavorable prognostic factor for all patients with gastric cancer (19). However, when considering MSC abundance in gastric cancer tissues, CPT1A became a favorable prognostic factor for patients with a decreased abundance of MSCs in gastric cancer tissues, but not for patients with an enriched MSC abundance status. These findings indicate a complex role of CPT1A in gastric cancer and the underlying mechanisms need to be further elucidated. High levels of the two miRNAs (miR-5572 and miR-6855-5p) were shown to be associated with the favorable prognosis of patients with a decreased number of MSCs, which suggests a potential link between the two miRNAs and MSCs in gastric cancer. Furthermore, apart from miR-5572, the other regulatory axis molecules were consistently altered in GC-MSCs and their expression exhibited a good correlation with each other in MSCs. The overall trend of miR-5572 expression changes was consistent with the prior findings (miR-5572 expression was downregulated in GC-MSCs), but without a significant difference. This discrepancy may be caused by their scattered expression in these selected MSCs. To further analyze the association between the regulatory axis molecules and to comprehensively evaluate the clinical implication of circ_024017, more clinical gastric cancer samples and GC-MSCs need to be included for further assessments.

In conclusion, the present study identified that circ_0024107, as a GC-MSC-derived novel circRNA, induced the FAO metabolic reprogramming of GC-MSCs via the miR-5572/6855-5p-CPT1A axis, which enables GC-MSC-CM to upregulate the circ_0024107 level in gastric cancer cells, thus increasing FAO activity through the same axis to enhance gastric cancer cell migration and invasion to form lymphatic metastasis (Fig. 8). These findings present novel insight into gastric cancer malignant progression and may lead to the development of potential therapeutic targets for gastric cancer.

**Acknowledgements**

Not applicable.

**Funding**

The present study was supported by the National Natural Science Foundation of China (grant nos. 81902510, 81772641 and 81972313), the Medical Scientific Research Project of Jiangsu Provincial Health Commission (grant no. Z2022022), the Suzhou Health Youth Backbone Talent of National Mentor System (grant no. ngg2021043) and the Postgraduate Research and Practice Innovation Program of Jiangsu Province (grant no. KYCX22_3719).

**Availability of data and materials**

The datasets used and/or analyzed during the current study are available from the corresponding author on reasonable request.

## Authors' contributions

LW, CW and JX performed the research and wrote the draft of the manuscript. ZG, XC and JH performed the statistical analyses and interpreted the data. XC and HD provided technical and material support, and contributed to the design of the study. WZ and FH performed critical revisions of the manuscript and were involved in design of the study. MW and CZ were involved in the conception and design of the study

## Ethics approval and consent to participate

The collection of tissues from gastric cancer patients was approved by the Affiliated Tumor Hospital of Nantong University (approval no. 2021-017). The animal experiment was approved by the Committee on Use and Care of Animals of Jiangsu University [approval no. SYXK(Su) 2018-0053].

## Patient consent for publication

Not applicable.

## Competing interests

The authors declare that they have no competing interests.

## References


1. Sung H, Ferlay J, Siegel RL, Laversanne M, Soerjomataram I, Jemal A and Bray F: Global cancer statistics 2020: GLOBOCAN estimates of incidence and mortality worldwide for 36 cancers in 185 Countries. CA Cancer J Clin 71: 209-249, 2021.
2. Quail DF and Joyce JA: Microenvironmental regulation of tumor progression and metastasis. Nat Med 19: 1423-1437, 2013.
3. Cao H, Xu W, Qian H, Zhu W, Yan Y, Zhou H, Zhang X, Xu X, Li J, Chen Z and Xu X: Mesenchymal stem cell-like cells derived from human gastric cancer tissues. Cancer Lett 274: 61-71, 2009.
4. Wang M, Zhao C, Shi H, Zhang B, Zhang L, Zhang X, Wang S, Wu X, Yang T, Huang F, *et al*: Deregulated microRNAs in gastric cancer tissue-derived mesenchymal stem cells: Novel biomarkers and a mechanism for gastric cancer. Br J Cancer 110: 1199-1210, 2014.
5. Huang F, Wang M, Yang T, Cai J, Zhang Q, Sun Z, Wu X, Zhang X, Zhu W, Qian H and Xu W: Gastric cancer-derived MSC-secreted PDGF-DD promotes gastric cancer progression. J Cancer Res Clin Oncol 140: 1835-1848, 2014.
6. Zhu M, Wang M, Yang F, Tian Y, Cai J, Yang H, Fu H, Mao F, Zhu W, Qian H and Xu W: miR-155-5p inhibition promotes the transition of bone marrow mesenchymal stem cells to gastric cancer tissue derived MSC-like cells via NF-κB p65 activation. Oncotarget 7: 16567-16580, 2016.
7. Sun L, Huang C, Zhu M, Guo S, Gao Q, Wang Q, Chen B, Li R, Zhao Y, Wang M, *et al*: Gastric cancer mesenchymal stem cells regulate PD-L1-CTCF enhancing cancer stem cell-like properties and tumorigenesis. Theranostics 10: 11950-11962, 2020.
8. Wang M, Chen B, Sun XX, Zhao XD, Zhao YY, Sun L, Xu CG, Shen B, Su ZL, Xu WR and Zhu W: Gastric cancer tissue-derived mesenchymal stem cells impact peripheral blood mononuclear cells via disruption of Treg/Th17 balance to promote gastric cancer progression. Exp Cell Res 361: 19-29, 2017.
9. Li W, Zhang X, Wu F, Zhou Y, Bao Z, Li H, Zheng P and Zhao S: Gastric cancer-derived mesenchymal stromal cells trigger M2 macrophage polarization that promotes metastasis and EMT in gastric cancer. Cell Death Dis 10: 918, 2019.
10. Sun L, Wang Q, Chen B, Zhao Y, Shen B, Wang H, Xu J, Zhu M, Zhao X, Xu C, *et al*: Gastric cancer mesenchymal stem cells derived IL-8 induces PD-L1 expression in gastric cancer cells via STAT3/mTOR-c-Myc signal axis. Cell Death Dis 9: 928, 2018.
11. Wang M, Gong Z, Zhao X, Yu W, Huang F and Dong H: Circular RNAs emerge as important regulators with great potential for clinical application in gastric cancer. Biomark Med 15: 69-82, 2021.
12. Shan C, Zhang Y, Hao X, Gao J, Chen X and Wang K: Biogenesis, functions and clinical significance of circRNAs in gastric cancer. Mol Cancer 18: 136, 2019.
13. Zhao L, Liu Y, Zhang S, Wei L, Cheng H, Wang J and Wang J: Impacts and mechanisms of metabolic reprogramming of tumor microenvironment for immunotherapy in gastric cancer. Cell Death Dis 13: 378, 2022.
14. Cui MY, Yi X, Zhu DX and Wu J: Aberrant lipid metabolism reprogramming and immune microenvironment for gastric cancer: A literature review. Transl Cancer Res 10: 3829-342, 2021.
15. Huo J, Guan J and Li Y: Metabolism reprogramming signature associated with stromal cells abundance in tumor microenvironment improve prognostic risk classification for gastric cancer. BMC Gastroenterol 22: 364, 2022.
16. Wang M, Zhao X, Qiu R, Gong Z, Huang F, Yu W, Shen B, Sha X, Dong H, Huang J, *et al*: Lymph node metastasis-derived gastric cancer cells educate bone marrow-derived mesenchymal stem cells via YAP signaling activation by exosomal Wnt5a. Oncogene 40: 2296-2308, 2021.
17. Livak KJ and Schmittgen TD: Analysis of relative gene expression data using real-time quantitative PCR and the 2(-Delta Delta C(T)) method. Methods 25: 402-408, 2001.
18. Ma Y, Temkin SM, Hawkridge AM, Guo C, Wang W, Wang XY and Fang X: Fatty acid oxidation: An emerging facet of metabolic transformation in cancer. Cancer Lett 435: 92-100, 2018.
19. Wang M, Yu W, Cao X, Gu H, Huang J, Wu C, Huang J, Wu C, Wang L, Sha X, *et al*: Exosomal CD44 transmits lymph node metastatic capacity between gastric cancer cells via YAP-CPT1A-mediated FAO reprogramming. Front Oncol 12: 860175, 2022.
20. Kim SJ, Khadka D and Seo JH: Interplay between solid tumors and tumor microenvironment. Front Immunol 13: 882718, 2022.
21. Pavlova NN and Thompson CB: The emerging hallmarks of cancer metabolism. Cell Metab 23: 27-47, 2016.
22. Dey P, Kimmelman AC and DePinho RA: Metabolic codependencies in the tumor microenvironment. Cancer Discov 11: 1067-1081, 2021.
23. Zhang X, Wang S, Wang H, Cao J, Huang X, Chen Z, Xu P, Sun G, Xu J, Lv J and Xu Z: Circular RNA circNRIP1 acts as a microRNA-149-5p sponge to promote gastric cancer progression via the AKT1/mTOR pathway. Mol Cancer 18: 20, 2019.
24. Tang W, Fu K, Sun H, Rong D, Wang H and Cao H: CircRNA microarray profiling identifies a novel circulating biomarker for detection of gastric cancer. Mol Cancer 17: 137, 2018.
25. Zhang Y, Feng Z, Xu Y, Jiang S, Zhang Q, Zhang Z, Wang K, Li X, Xu L, Yuan M, *et al*: Novel roles of LSECtin in gastric cancer cell adhesion, migration, invasion, and lymphatic metastasis. Cell Death Dis 13: 593, 2022.
26. Zheng S, Hu C, Lin H, Li G, Xia R, Zhang X, Su D, Li Z, Zhou Q, Chen R, *et al*: circCUL2 induces an inflammatory CAF phenotype in pancreatic ductal adenocarcinoma via the activation of the MyD88-dependent NF-κB signaling pathway. J Exp Clin Cancer Res 41: 71, 2022.
27. Ba L, Xue C, Li X, Zhang M, Yang Y, Han Q, Sun Z and Zhao RC: Gastric cancer cell-derived exosomes can regulate the biological functions of mesenchymal stem cells by inducing the expression of circular RNA circ_0004303. Stem Cells Dev 30: 830-842, 2021.
28. Wu H, Liu B, Chen Z, Li G and Zhang Z: MSC-induced lncRNA HCP5 drove fatty acid oxidation through miR-3619-5p/AMPK/PGC1alpha/CEBPB axis to promote stemness and chemo-resistance of gastric cancer. Cell Death Dis 11: 233, 2020.
29. He W, Liang B, Wang C, Li S, Zhao Y, Huang Q, Liu Z, Yao Z, Wu Q, Liao W, *et al*: MSC-regulated lncRNA MACC1-AS1 promotes stemness and chemoresistance through fatty acid oxidation in gastric cancer. Oncogene 38: 4637-4654, 2019.
30. Chen L and Shan G: CircRNA in cancer: Fundamental mechanism and clinical potential. Cancer Lett 505: 49-57, 2021.
31. Yu T, Wang Y, Fan Y, Fang N, Wang T, Xu T, Xu T and Shu Y: CircRNAs in cancer metabolism: A review. J Hematol Oncol 12: 90, 2019.
32. Wu H, Xu J, Gong G, Zhang Y and Wu S: CircARL8B contributes to the development of breast cancer via regulating miR-653-5p/HMGA2 axis. Biochem Genet 59: 1648-1665, 2021.
33. Chen Q, Yang Z, Ding H, Li H, Wang W and Pan Z: CircWHSC1 promotes breast cancer progression by regulating the FASN/AMPK/mTOR axis through sponging miR-195-5p. Front Oncol 11: 649242, 2021.